

Infection and Immunity

Identification and Characterization of Small Molecules That Inhibit Intracellular Toxin Transport

Jose B. Saenz, Teresa A. Doggett and David B. Haslam
Infect. Immun. 2007, 75(9):4552. DOI: 10.1128/IAI.00442-07.
Published Ahead of Print 18 June 2007.

Updated information and services can be found at:
<http://iai.asm.org/content/75/9/4552>

SUPPLEMENTAL MATERIAL

These include:

[Supplemental material](#)

REFERENCES

This article cites 64 articles, 38 of which can be accessed free
at: <http://iai.asm.org/content/75/9/4552#ref-list-1>

CONTENT ALERTS

Receive: RSS Feeds, eTOCs, free email alerts (when new
articles cite this article), [more»](#)

Information about commercial reprint orders: <http://journals.asm.org/site/misc/reprints.xhtml>
To subscribe to to another ASM Journal go to: <http://journals.asm.org/site/subscriptions/>

Journals.ASM.org

Identification and Characterization of Small Molecules That Inhibit Intracellular Toxin Transport^{∇†}

Jose B. Saenz, Teresa A. Doggett, and David B. Haslam*

Departments of Pediatrics and Molecular Microbiology, Washington University School of Medicine, St. Louis, Missouri 63110

Received 26 March 2007/Returned for modification 24 April 2007/Accepted 7 June 2007

Shiga toxin (Stx), cholera toxin (Ctx), and the plant toxin ricin are among several toxins that reach their intracellular destinations via a complex route. Following endocytosis, these toxins travel in a retrograde direction through the endosomal system to the *trans*-Golgi network, Golgi apparatus, and endoplasmic reticulum (ER). There the toxins are transported across the ER membrane to the cytosol, where they carry out their toxic effects. Transport via the ER from the cell surface to the cytosol is apparently unique to pathogenic toxins, raising the possibility that various stages in the transport pathway can be therapeutically targeted. We have applied a luciferase-based high-throughput screen to a chemical library of small-molecule compounds in order to identify inhibitors of Stx. We report two novel compounds that protect against Stx and ricin inhibition of protein synthesis, and we demonstrate that these compounds reversibly inhibit bacterial transport at various stages in the endocytic pathway. One compound (compound 75) inhibited transport at an early stage of Stx and Ctx transport and also provided protection against diphtheria toxin, which enters the cytosol from early endosomes. In contrast, compound 134 inhibited transport from recycling endosomes through the Golgi apparatus and protected only against toxins that access the ER. Small-molecule compounds such as these will provide insight into the mechanism of toxin transport and lead to the identification of compounds with therapeutic potential against toxins routed through the ER.

Bacterial and plant toxins are significant agents of human disease and potential vehicles for bioterrorism. Though their intracellular targets are diverse, a common and essential step in their virulence is the ability to reach the cytosol, where most toxins exert their enzymatic effects. The bacterial exotoxins Shiga toxin (Stx) and cholera toxin (Ctx), as well as the plant toxin ricin, have drawn particular interest for their unique retrograde transport following endocytosis. Members of the AB toxin group, these toxins consist of a receptor-binding B subunit and an enzymatic A subunit. In contrast to anthrax and diphtheria toxins, AB toxins that enter the cytosol directly from early endosomes in a pH-dependent manner (18, 28, 35), these membrane-bound toxins bypass the late endocytic pathway by retrograde transport from early or sorting endosomes to the *trans*-Golgi network (TGN) (14, 15, 37, 60). From the TGN, they traffic through the Golgi apparatus to the endoplasmic reticulum (ER), where they are subsequently translocated through the Sec61p channel into the cytosol via ER quality control mechanisms (49, 56, 62). It is believed that this complex retrograde transport may allow for certain essential steps in toxin activation and transfer; Stx has been shown to be cleaved and activated by host proteases (16). Similarly, the ability to reach the ER may enable a chaperone-facilitated transfer to the cytosol, as previously reported for Ctx, ricin, and Stx (49, 52, 62, 63).

The existence of a retrograde transport pathway was first uncovered by electron microscopic studies tracking the intra-

cellular transport of Stx (46). Since that time, a number of toxins, in addition to Ctx and ricin, have likewise been found to transit through the ER en route to the cytoplasm. Given the importance of these pathways to intoxication by diverse pathogenic agents, a number of investigations have been directed at identifying host molecules involved in toxin transport. Previous studies aimed at identifying essential components of the retrograde pathways of Stx, ricin, and Ctx have focused largely on the Rab family of small GTP-binding proteins. Members of the Rab family cycle between their GTP- and GDP-bound forms, which are related to their functions as regulators of vesicular traffic (53). Standard genetic approaches involving overexpression of dominant-negative mutants or small interfering RNA knockdowns of various Rabs have revealed the complexity of toxin trafficking pathways. Inhibition of Rab7 and Rab9, which are involved in lysosome targeting pathways, had no effect on ricin and Stx trafficking (21, 47). In contrast, inhibition of Rab6a', involved in endosome-to-TGN transport, inhibited Stx transport from endosomes through the Golgi apparatus (17, 33, 59) but had no effect on ricin transport or intoxication (8). Similarly, overexpression of a dominant-negative Rab11, implicated in transport from recycling endosomes to the TGN, resulted in impaired Stx transport but had no effect on ricin (21, 60). Rab22, like Rab6a', has been implicated in endosome-to-TGN transport, though inhibition of Rab22 function has had inconsistent effects on retrograde toxin transport (34). Though these pathways still remain poorly characterized, the sequential retrograde progression utilized by these toxins has translated into a unique system for probing host endocytic mechanisms.

In an effort to dissect and inhibit the stepwise trafficking of Stx, we have developed a quantitative and highly sensitive, high-throughput luciferase-based assay to screen a library of small-molecule compounds for their ability to block Stx-medi-

* Corresponding author. Mailing address: Departments of Pediatrics and Molecular Microbiology, Washington University School of Medicine, St. Louis, MO 63110. Phone: (314) 286-2888. Fax: (314) 286-2895. E-mail: haslam@kids.wustl.edu.

† Supplemental material for this article may be found at <http://iai.asm.org/>.

∇ Published ahead of print on 18 June 2007.

ated inhibition of protein synthesis (64). Because Stx transport involves a multistep progression through the cell, we predicted that inhibitory compounds could be identified at distinct stages along the retrograde trafficking pathway and could potentially be directed at specific molecular targets. From an initial screen of 14,400 small compounds, we identified several potential inhibitors. Among these, we characterized two compounds (compounds 75 and 134) that reversibly inhibit Shiga intoxication and act at distinct steps along the toxin trafficking pathway. Our results demonstrate the utility of a small-molecule approach to elucidating toxin transport pathways and will lead to the identification of novel therapeutic approaches targeting diseases caused by ER-routed toxins.

MATERIALS AND METHODS

Reagents and antibodies. Small chemical compounds were purchased from ChemDiv and reconstituted to 5-mg/ml stocks in dimethyl sulfoxide (DMSO). All compounds were checked for purity by mass spectroscopy. Shiga-like toxin 1 and diphtheria toxin (DT) were from List Biological Laboratories, and ricin was from Sigma. Recombinant Ctx subunit B (CtxB) labeled with Alexa Fluor 488, Alexa Fluor 594-labeled human transferrin (Tf), SlowFade Gold mounting reagent with or without 4',6'-diamidino-2-phenylindole (DAPI), and Alexa Fluor-labeled goat or donkey secondary antibodies against immunoglobulin G were obtained from Molecular Probes. Rabbit anti-giantin was from Covance and sheep anti-human TGN46 from Serotec. Dulbecco's modified Eagle's medium (DMEM), Eagle's minimum essential medium, streptomycin, and penicillin were from BioWhittaker. Nonessential amino acids were purchased from Mediatech. Cycloheximide, DMSO, brefeldin A (BFA), nocodazole, anisomycin, and staurosporine were from Sigma. Tran³⁵S was purchased from MP Biomedicals, and ³⁵S-labeled O₄ was obtained from American Radiolabeled Chemicals.

Cell culture. Vero cells were grown and maintained in DMEM supplemented with 10% fetal calf serum (Sigma), 100 µg/ml streptomycin, 100 U/ml penicillin, and 1% nonessential amino acids at 37°C under 5% CO₂.

Purification of StxB. The recombinant B subunit of Stx (StxB) was isolated from periplasmic extracts of *Escherichia coli* BL21(DE3) cells (Invitrogen) containing the pT7B5-1 expression vector, as previously described (11). Briefly, periplasmic extracts were subjected to anion-exchange chromatography on a Q-Sepharose column (Pharmacia), and pentameric StxB was isolated following further purification of the Q-Sepharose peak on a Superdex 75R 10/30 gel filtration column (Pharmacia). Fractions containing StxB were identified by slot blot (Hoefer) using a polyclonal rabbit anti-StxB antibody (11), and positive fractions were combined and concentrated to 1 mg/ml using Ventricon Plus-20 filters (Millipore). StxB purity was verified by sodium dodecyl sulfate (SDS)-polyacrylamide gel electrophoresis on a 4 to 20% Tris-HCl gel stained with Coomassie blue. Alexa Fluor 488 and 594 conjugation was performed by following the manufacturer's recommendations (Molecular Probes).

Luciferase-based assay for measuring protein synthesis. The luciferase-based assay has been described previously (64). It was applied to a high-throughput screen (HTS) of small molecules consisting of known biological compounds as well as unknown compounds at the ICCB facility at Harvard University. The luciferase protein has been modified by Promega by the addition of a PEST sequence, resulting in its short intracellular half-life (44). The luciferase-PEST cDNA was cloned into an adenovirus expression plasmid (64), and high-titer viral stocks were generated (pAD-Luc). Vero cell monolayers were transduced with pAD-Luc (multiplicity of infection, 200), incubated for 24 h at 37°C under 5% CO₂, and then seeded into 384-well black polystyrene plates (Corning) at 1 × 10⁴ cells/well for an additional 24 h. Cells were then treated for 30 min at 37°C with known biological compounds and unknown compounds at 5 mg/ml. Stx was added at 1 ng/ml, and cells were incubated for an additional 4 h at 37°C. To determine luciferase expression, the SuperLight luciferase reporter gene assay was used according to the manufacturer's instructions (BioAssay Systems), and light output was detected using an LMax 1.1L luminometer (Molecular Devices). To be considered protective, the compound must increase the luciferase signal at least twofold above the mean observed from cells treated with toxin alone. Compounds maintaining luciferase expression levels in the presence of cycloheximide alone (100 µg/ml) were excluded from further analysis.

Radioactive amino acid incorporation assay. Experiments measuring radioactive ³⁵S incorporation were used to confirm positive hits from the luciferase-based HTS. This assay was adapted to a multiwell format to enable testing on a

large number of samples. Vero cells were cultured overnight at 37°C under 5% CO₂ in 96-well plates at 2.5 × 10⁴ cells/well, whereupon the medium was removed and replaced with either prewarmed medium (plus 0.5% [vol/vol] DMSO) or a medium containing a compound. Following a 1-h incubation at 37°C, toxin was added to wells in triplicate, and cells were shifted to 37°C for an additional 4 h. The medium was then removed from all wells and replaced with a medium containing Tran³⁵S-label at 10 µCi/ml. Cells were incubated at 37°C for 45 min, washed with phosphate-buffered saline (PBS) (pH 7.4), and lysed (1 mg/ml bovine serum albumin, 0.2% deoxycholic acid, 0.1% SDS, 20 mM Tris [pH 7.4]) at 4°C for 12 h. Proteins from the lysed cells were precipitated with trichloroacetic acid (TCA) (final concentration, 15%) and transferred to multiscreen HA plates (Millipore), and the filters were washed with ice-cold 20% TCA. Filters were then removed from the plate and placed in 2 ml Bio-Safe II scintillation fluid (RPI), and ³⁵S incorporation was quantitated using a beta counter (Beckman). Independent experiments were performed at least three times for potent compounds, and data were analyzed using Prism software (version 4.0; 2003).

Toxin and Tf internalization. For toxin trafficking experiments, Vero cells were grown in chamber slides (2.5 × 10⁴ cells/chamber), treated with a medium containing DMSO, compound, or known agents at the indicated concentrations for 1 h at 37°C, and then placed on ice for 15 min prior to the addition of toxin. The toxin was bound for 45 min at 4°C, followed by washing of unbound toxin with ice-cold PBS (pH 7.4). Fresh, prewarmed medium was added, and cells were shifted to 37°C for the indicated times to allow for toxin internalization. In Tf trafficking experiments, cells were pretreated with compounds in serum-free culture medium, and Tf and toxin were bound to cells at 4°C for 1 h, followed by a shift to 22°C for 1 h. For all immunofluorescence experiments, cells were fixed in 4% paraformaldehyde in cold PBS, permeabilized in a culture medium containing 0.1% Triton X-100, and blocked with a culture medium containing 0.1% bovine serum albumin (wt/vol), all at room temperature. All primary antibodies and secondary antibodies (donkey anti-immunoglobulin G labeled with Alexa Fluor 488, 594, or 555) were diluted in blocking buffer. Cells were rinsed thoroughly in PBS prior to being mounted in SlowFade Gold reagent with or without DAPI (Invitrogen Corp.). Fluorescence imaging used epifluorescence (Zeiss) or confocal (Olympus) microscopy.

Cell viability assay. The viability of cells treated with a compound was evaluated using the CellTiter-Glo luminescent cell viability assay (Promega), a luciferase-based assay. Vero cells (5 × 10⁴/well) were added to 96-well plates and grown at 37°C under 5% CO₂ overnight. The medium was then removed and replaced with a prewarmed medium either with DMSO alone or with a compound, in triplicate. Following incubation at 37°C for various times, an equal volume of CellTiter reagent (50 µl) was added according to the manufacturer's instructions, and the light output was measured using the Lmax 1.1L luminometer. Independent experiments were performed three times.

Cloning and expression of StxB-Sulf₂-His₆. In order to add overlapping sulfation sites to the carboxyl terminus of StxB, the StxB gene from pNAS-13 (11) was amplified with primers Sulf-1 (5'-GGTGTCAAGGAGTATTGTGTAATATGAAAAAACATTATTAATAGC-3') and Sulf-2 (5'-GGATTACAGCGAA GTTATTTTCGTGGAGAGGAACCTGAGTATGGAGAGAGGAACCTGAGTATGGAGAAAAGCGGCCGAAAAAAGTAGGCCG-3'), which encodes the two overlapping sulfation sites (Sulf₂) added to StxB by Johannes et al. (22). The amplified product was ligated into expression plasmid pCRT7-TOPO (Invitrogen). Sequencing of one such product revealed a nucleotide deletion at base 312 of the StxB coding region, such that the sulfation sites were intact and the frameshift resulted in read-through in frame into the pCRT7 flanking sequence encoding a V5 epitope, a histidine tag, and a stop codon. This protein was found to be expressed at a high level from BL21(DE3) cells and was used in further studies. The protein was expressed from BL21(DE3) cells by the addition of 0.1 M isopropyl-β-D-thiogalactopyranoside (IPTG) (Fisher Scientific) to cultures growing at late-log phase. After 2 h of incubation at 30°C, the bacteria were harvested by centrifugation, and a periplasmic extract was prepared by osmotic lysis. The material was mixed with 2 ml of nickel-nitrilotriacetic acid resin (QIAGEN) and incubated overnight at 4°C with rocking. The resin and periplasmic extract were then applied to an empty column, and the beads were washed with several column volumes of PBS, followed by PBS containing imidazole at 25, 50, 250, and 500 mM. The StxB-Sulf₂-His protein, which remained associated with the column at 500 mM imidazole, was released by the addition of 5 ml of 2 M imidazole in PBS. The eluted protein was dialyzed twice against PBS (pH 7.4), aliquoted, and stored at 4°C. In order to demonstrate that addition of the sulfation, V5, and histidine tags did not affect the binding and transport of the toxin, StxB-Sulf₂-His was labeled with Alexa Fluor 488 according to the manufacturer's instructions (Molecular Probes). Vero cells were incubated with 1 µg/ml each of StxB-Sulf₂-His-Alexa Fluor 488 and wild-type StxB labeled with Alexa Fluor 594. After binding at 4°C for 1 h, the cells were washed, warmed to

37°C for 1 h, fixed with 4% paraformaldehyde, and visualized by epifluorescence microscopy.

Sulfation of StxB-Sulf₂-His. Vero cells were seeded overnight at 37°C under 5% CO₂ (1 × 10⁶ cells/well). The next day, the medium was replaced with serum-free DMEM lacking sulfate (Washington University Tissue Culture Support Center), and cells were incubated for an additional 3.5 h at 37°C. The medium was replaced with sulfate-free DMEM containing DMSO or compound for 30 min at 37°C; then it was replaced with prewarmed sulfate-free medium containing 1 mCi/ml ³⁵S-labeled O₄ for 3 h at 37°C. Wells were washed with cold PBS (pH 7.4) and lysed with PBS containing 1% Triton X-100. The protein concentrations of postnuclear supernatants were determined by the bicinchoninic acid protein assay kit (Pierce), and 250 μg of lysates was added to 40 μl of nickel-nitrilotriacetic acid Superflow beads and rotated at 4°C overnight. The next day, beads were spun down at 5,000 rpm for 5 min, and the unbound fraction was collected. Total ³⁵S-incorporated counts were determined by measuring radioactive counts from TCA-precipitated proteins of unbound lysates. Beads were washed once with PBS containing 1% Triton X-100 and twice with PBS. Beads were resuspended in imidazole (1.5 M in PBS), and eluates were denatured with 1× SDS gel-loading buffer (50 mM Tris-HCl, 100 mM β-mercaptoethanol, 2% SDS, 0.1% bromophenol blue, 10% [vol/vol] glycerol) and boiled. Eluates were resolved on a 10 to 20% Tris-HCl denaturing gel, fixed, and developed overnight in a phosphorimager cassette.

Expression and trafficking of VSVG-GFP. Vero cells were transiently transfected with vesicular stomatitis virus G protein (VSVG)-green fluorescent protein (GFP) ts045, as previously described for other cell lines (19). Briefly, 10⁶ Vero cells were transfected with 20 μg of pCDM8.1 expressing VSVG-GFP ts045 and a Lipofectamine 2000 (Invitrogen) mixture in antibiotic-free medium (DMEM with 10% fetal calf serum), followed by overnight incubation at 37°C under 5% CO₂. Cells were collected and placed in chamber slides (Lab-Tek) for an additional 8 to 10 h at 37°C before their transfer to 42°C for 12 to 16 h. Cells were then treated with compounds or BFA (25 μg/ml) in prewarmed, antibiotic-free medium for 1 h at 42°C before being transferred to 32°C. Thirty minutes prior to the shift to 32°C, all chambers were treated with cycloheximide (100 μg/ml) to prevent de novo protein synthesis. Cells were fixed following various incubation times at 32°C. Fixation, permeabilization, staining, and imaging were performed as described for toxin and Tf internalization experiments.

GFP secretion time course. A plasmid encoding enhanced GFP (EGFP) fused at the amino terminus with the secretion signal of human neuropeptide Y (NPY) was obtained from Richard Mains (12). The insert was released by BglII and NotI digestion and ligated into plasmid pENTR-4 (Invitrogen) that had been digested with BamHI and NotI. This plasmid was used as the source for insertion of the NPY-EGFP cDNA into adenovirus expression plasmid pAD-DEST (Invitrogen) by the clonease reaction (Invitrogen). The resulting plasmid, pAD-NPY-GFP, was linearized with PacI and transfected into 293A cells to prepare a low-titer viral stock. The virus was amplified by further passage in 293A cells until a high-titer stock was prepared. Vero cells transduced with pAD-NPY-GFP were washed, trypsinized, and seeded into 8-well chamber slides. The next day, the medium was replaced with a culture medium containing DMSO or the indicated compound for 30 min at 37°C. Cycloheximide was then added at 100 μg/ml, and cells were washed and fixed with 4% paraformaldehyde in PBS (pH 7.4) at various times following cycloheximide treatment. Permeabilization, staining, and imaging were performed as described for toxin and Tf internalization experiments.

Assessment of NPY-GFP secretion. Approximately 5 × 10⁶ Vero cells were infected overnight at 37°C under 5% CO₂ with pAD-NPY-GFP. Cells were then washed, trypsinized, and seeded into each well of a 6-well plate (~1 × 10⁶ cells/well). The next day, the medium was removed, and cells were washed twice with serum-free medium. The medium was subsequently replaced with serum-free DMEM containing DMSO or a compound for 30 min at 37°C. Cells were all treated with cycloheximide (100 μg/ml) to inhibit de novo protein synthesis and to synchronize NPY-GFP trafficking. At various time points following cycloheximide treatment, supernatants were collected, and GFP secretion was assessed by an enzyme-linked immunosorbent assay (ELISA) as described in the manufacturer's instructions (Pierce). ELISA plates were analyzed by the Gen5 software program (BioTek) using the Synergy 2 spectrophotometer (BioTek). The mean absorbance for control wells containing DMEM alone was subtracted from the absorbance for each sample well before analysis.

Statistics. All statistical analyses were performed by GraphPad Prism 5. For Fig. 1, toxin concentrations were log transformed prior to curve fitting and statistical analyses. Toxin-response curves were generated by nonlinear regression (least-squares fit) to correspond to the observed data, and the concentration of toxin needed to reduce protein synthesis by 50% (50% inhibitory concentration [IC₅₀]) was calculated by using the fitted curves. For the toxin-response

curves, the toxin concentration varied, while the concentration of DMSO (0.5% [vol/vol] in control cells), compound 75 (25 μM), or compound 134 (50 μM) was kept constant. Toxin IC₅₀s were compared using the extra sum-of-squares *F* test applied to the best-fit curves for the data. Differences between toxin IC₅₀s were considered statistically significant at a *P* value of ≤0.05 and highly statistically significant at a *P* value of ≤0.01.

RESULTS

HTS for compounds that inhibit Stx activity in host cells.

Several toxins damage host cells by inhibiting protein synthesis. DT and *Pseudomonas* exotoxin inhibit protein synthesis through the ADP-ribosylation of elongation factor 2 (7, 41), whereas Stx and the plant toxin ricin inhibit ribosome function by cleaving an adenosine residue from the 60S ribosome (3, 13, 39, 40, 45). Still other toxins, such as Ctx and anthrax edema toxin, induce increases in second-messenger levels, resulting in cytotoxicity (6, 26, 54). In order to quantitate the effects of various protein synthesis-inhibiting toxins on host cells, we had previously established a luciferase-based assay that could readily determine the susceptibilities of various cell lines to Stx, ricin, DT, and *Pseudomonas* exotoxin (64). In cells constitutively expressing an mRNA encoding destabilized firefly luciferase, luciferase enzyme activity served as a surrogate measure of protein synthesis.

This assay was adapted to an HTS and applied to a screen of small-molecule compounds that inhibit toxin susceptibility. The ICCB facility at Harvard University contains a number of commercial libraries consisting of synthetic and natural products. An initial screen of biological compounds with known effects yielded positive hits such as BFA and D,L-threo-1-phenyl-2-decanoylamino-3-morpholino-1-propanol (PDMP) (data not shown), two compounds previously shown to inhibit Stx susceptibility through distinct mechanisms (25, 50) and serving as positive controls for the detection of Stx-inhibitory compounds. In addition, the assay detected known inhibitors of the proteasome, such as MG-132 (3). This was an expected result, since the discriminatory power of the assay is dependent on the rapid degradation of luciferase following translation (65).

We next screened the ChemDiv 3 library at the ICCB facility, consisting of 14,400 compounds of unknown function. The compounds included in this library were selected for their structural diversity, chemical stability, and "drug-like properties." Since these compounds were commercially available and their functions currently undefined, we reasoned that novel inhibitors could be identified. Among these were selected the top 1% of compounds yielding the highest luciferase signal in the presence of toxin, all of which resulted in a signal at least twice the baseline. Because the initial screen lacked a counterscreen to exclude compounds affecting luciferase turnover, each compound was subsequently tested for its effect on the luciferase signal following cycloheximide treatment. Cycloheximide-mediated inhibition of protein synthesis is independent of intracellular transport, and its mechanism of ribosomal inactivation is distinct from that of Stx (55). Therefore, compounds that provide protection against cycloheximide-mediated inhibition of the luciferase signal must be acting in a toxin-independent manner (e.g., by inhibiting luciferase degradation), and such compounds were excluded from further analysis. After exclusion of compounds that affected cycloheximide-induced suppression of the luciferase signal, eight com-

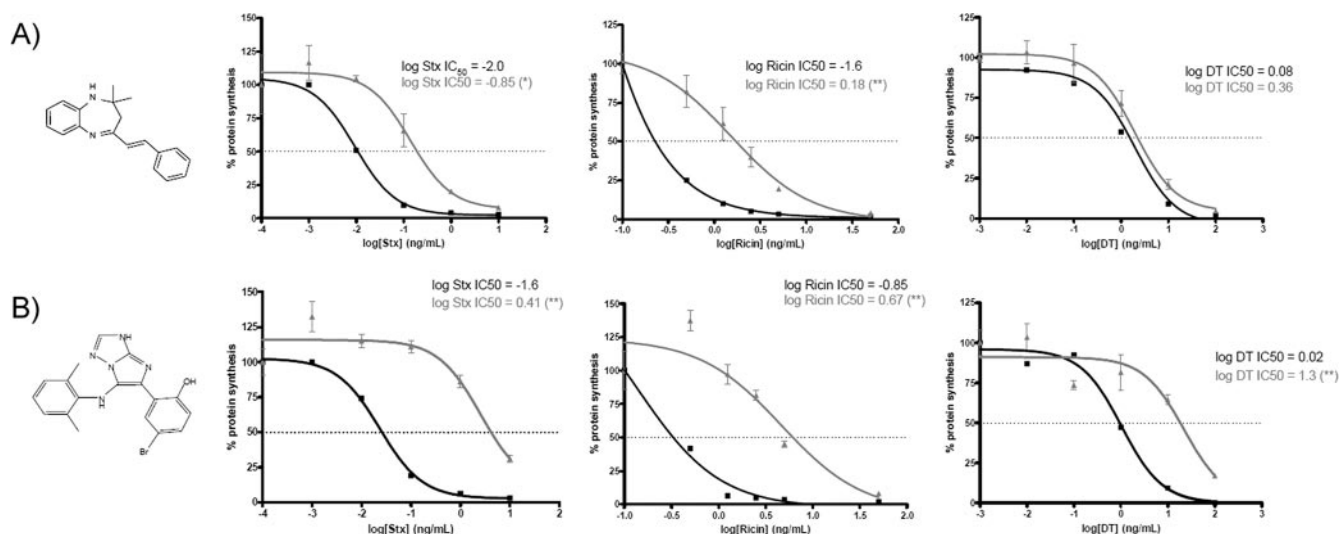


FIG. 1. Protective effects of inhibitory compounds against Stx, ricin, and DT. (A) Compound 134 structure and demonstration that this compound (50 μ M) protects against Stx- and ricin- but not DT-mediated decreases in protein synthesis. Toxin IC₅₀s for Stx and ricin in compound-treated cells were found to be statistically different (*, $P < 0.05$) from those in control cells. The DT IC₅₀ in compound-treated cells was not statistically different from that in control cells ($P > 0.05$). (B) Compound 75 structure and demonstration that this compound (25 μ M) protects against Stx-, ricin-, and DT-mediated decreases in protein synthesis. Toxin IC₅₀s for all three toxins in compound-treated cells were found to be highly statistically different (**, $P < 0.01$) from those in control cells. Protein synthesis levels for control (black squares) (no compound) and compound-treated (gray triangles) Vero cells were determined using the radioactive amino acid incorporation assay as described in Materials and Methods. The percentage of protein synthesis is expressed as the amount of radioactive amino acid incorporation in control or compound-treated cells at a given toxin concentration as a percentage of radioactive amino acid incorporation in cells lacking toxin treatment. Toxin-response curves, toxin IC₅₀s, and statistical comparisons between control and compound-treated cells were calculated as described in Materials and Methods. Each data point (mean \pm standard deviation) represents triplicate data at the indicated toxin concentration from one representative experiment.

pounds with toxin-specific effects were selected for further analysis. Notably, our subsequent screens have incorporated a cycloheximide counterscreen in order to exclude compounds with toxin-independent effects prior to secondary analysis (see Fig. S1 in the supplemental material).

Secondary analysis to determine the potency and efficacy of inhibitory compounds. The optimal protective concentration for each identified hit was determined using a radioactive assay for protein synthesis (11) that was modified for medium-throughput analysis in a multiwell format (see Materials and Methods). Since some of these compounds could exhibit non-specific effects at increased concentrations, the lowest concentration providing significant protection against Stx compared to the effect of the toxin on untreated Vero cells was considered to be optimal. Compounds classified as inhibitors showed half-maximal activity between 10 and 50 μ M (data not shown). Compounds were used above their half-maximal but below their maximal concentrations for all subsequent assays (at 25 μ M for compound 75 and 50 μ M for compound 134).

The abilities of these compounds to protect against increasing Stx concentrations were expressed as the toxin IC₅₀s (see Materials and Methods). Using these criteria, compounds 75 and 134, at their respective optimal concentrations, exhibited the greatest protective effects among the hits identified from the initial screen. Both compounds showed statistically significant increases in the Stx IC₅₀ compared to that for cells containing no compound (Fig. 1). At higher concentrations (50 μ M and 100 μ M, respectively), compounds 75 and 134 exhibited up to 1,000-fold increases in the Stx IC₅₀ (data not shown).

Neither of these compounds affected luciferase degradation in the presence of cycloheximide (data not shown).

An initial characterization of compounds showing highly protective effects against Stx led us to consider whether these compounds could protect against other toxins that inhibit protein synthesis. Compounds 75 and 134 showed similar statistically significant increases in the ricin IC₅₀ (Fig. 1) ($P < 0.01$). Protection against both Stx and ricin was also greater than the previously observed protective effects of an overexpressed dominant-negative mutant of Rab6, a small GTP-binding protein found to be essential to Stx transport through the Golgi apparatus (8).

Interestingly, compound 134 failed to show a statistically significant effect against DT-mediated protein synthesis inhibition (Fig. 1A), while compound 75 demonstrated greater protection (Fig. 1B). Vero cells that were not treated with a compound demonstrated a DT susceptibility profile similar to those for Stx and ricin. Stx and ricin, following endocytosis, are known to traffic from an endosomal compartment to the ER via the Golgi apparatus (30). DT, however, directly accesses the cytosol from early endosomes; the low endosomal pH is believed to allow for a conformational change in the holotoxin and to promote shuttling of the A moiety across the endosomal membrane (41). The lack of protection against DT suggests that compound 134 affects toxin transport at a point after the early-endosome stage but has no effect on trafficking from the plasma membrane to the early endosomal compartment. In contrast, the protective effect of compound 75 against all three toxins suggests that this compound affects transport mecha-

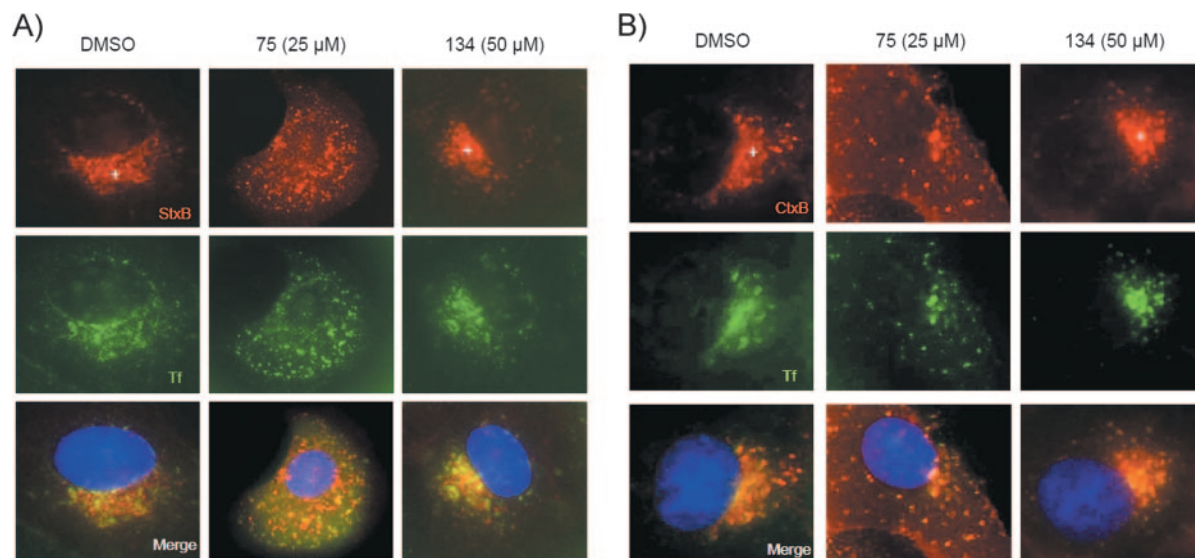


FIG. 2. Compound 75 impedes StxB/CtxB and Tf ligand trafficking to recycling endosomes. (A) Vero cells were first incubated with Alexa Fluor 594-labeled StxB (1 $\mu\text{g}/\text{ml}$) and Alexa Fluor 488-labeled Tf (1 $\mu\text{g}/\text{ml}$) for 1 h at 4°C in serum-free medium, then shifted to 22°C for an additional hour, and finally developed for immunofluorescence, as described in Materials and Methods. In control (0.5% [vol/vol] DMSO) and compound 134-treated cells, StxB reached a perinuclear, Tf-positive compartment previously described as recycling endosomes (cross). In compound 75-treated cells, however, no perinuclear staining was observed, and Tf and StxB were confined to early endosomes (punctate staining). (B) Neither CtxB nor Tf reached the perinuclear Tf-positive recycling endosome compartment in compound 75-treated Vero cells compared to control and compound 134-treated cells. Results are representative of two similar experiments. Images were obtained at $\times 1,000$ magnification. Blue, nuclei.

nisms common to all three pathways, presumably at an earlier stage in endocytosis than the site of action of compound 134.

Effects of compounds 75 and 134 on toxin transport. In order to determine the site at which inhibitory compounds were affecting toxin activity, the endocytosis and transport of fluorescent StxB and CtxB were examined. The retrograde transport of protein toxins is believed to occur exclusively from early and/or recycling endosomes (32). In order to determine whether endocytosis and trafficking of StxB to early and recycling endosomes were affected by compound 134, StxB transport was compared to that of fluorescently labeled Tf, which is known to accumulate in recycling endosomes at 22°C due to a block in recycling-endosome-to-TGN transport at this temperature (33). In agreement with previous reports, StxB colocalized with Tf-positive compartments in control cells at 22°C (Fig. 2A). StxB trafficking to Tf-positive compartments in compound 134-treated cells was not significantly different from that in control cells, showing a similar level of colocalization with the perinuclear recycling-endosome compartment (Fig. 2A). Similar results were seen with CtxB, which also accumulated in a Tf-positive perinuclear compartment. (Fig. 2B). In addition, compound 134 did not affect the binding of StxB to the cell surface (see Fig. S2 in the supplemental material), suggesting that this compound was not occupying toxin receptor binding sites or significantly decreasing receptor expression. Taken together with the relative lack of protection by compound 134 against DT-mediated protein synthesis inhibition (Fig. 1A), these results collectively suggest that compound 134 maintains Stx and Ctx transport to recycling endosomes.

Compound 75, like compound 134, did not inhibit StxB binding to its receptor or decrease receptor expression (see Fig. S2 in the supplemental material). However, treatment with compound 75 appeared to inhibit the transport of both

StxB/CtxB and Tf to perinuclear recycling endosomes. Most of the toxin and most of the Tf were located in peripheral vesicular structures (Fig. 2A and B), likely early endosomes. These results, in addition to those demonstrating the effects of compound 75 on susceptibility to DT, collectively suggest that this compound inhibits Stx and Ctx transport to recycling endosomes.

Immunohistochemical analysis of compound-treated cells revealed morphological changes to the Golgi apparatus (see Fig. S3 in the supplemental material). The dispersal of the Golgi apparatus is a morphological effect that has been observed under several conditions that impair retrograde and intra-Golgi transport (10). To exclude the possibility that the effects of these compounds were not specific to intracellular toxin transport, we sought to rule out processes that are known to have effects on Golgi morphology. In particular, during the process of apoptosis, the Golgi apparatus becomes fragmented (9, 31, 43). In order to rule out the possibility that compounds 75 and 134 were inducing Golgi apparatus fragmentation through apoptosis, ATP levels in compound-treated cells were compared to those in untreated cells or cells treated with staurosporine, a known apoptosis-inducing agent (23). Treatment with compound 75 or 134 failed to deplete ATP levels over 24 h, in contrast to the effect observed following staurosporine treatment, suggesting that the compounds were not cytotoxic or apoptosis inducing at the specified concentrations over the time course studied (Fig. 3A). In addition, compound-treated cells consistently showed a more punctate and swollen Golgi apparatus compared to the more tubulated Golgi apparatus in staurosporine-treated cells (Fig. 3B). The Golgi morphology of compound-treated cells also differed from the characteristic Golgi architecture of cells treated with anisomycin, a peptidyl transferase inhibitor shown to induce apoptosis in

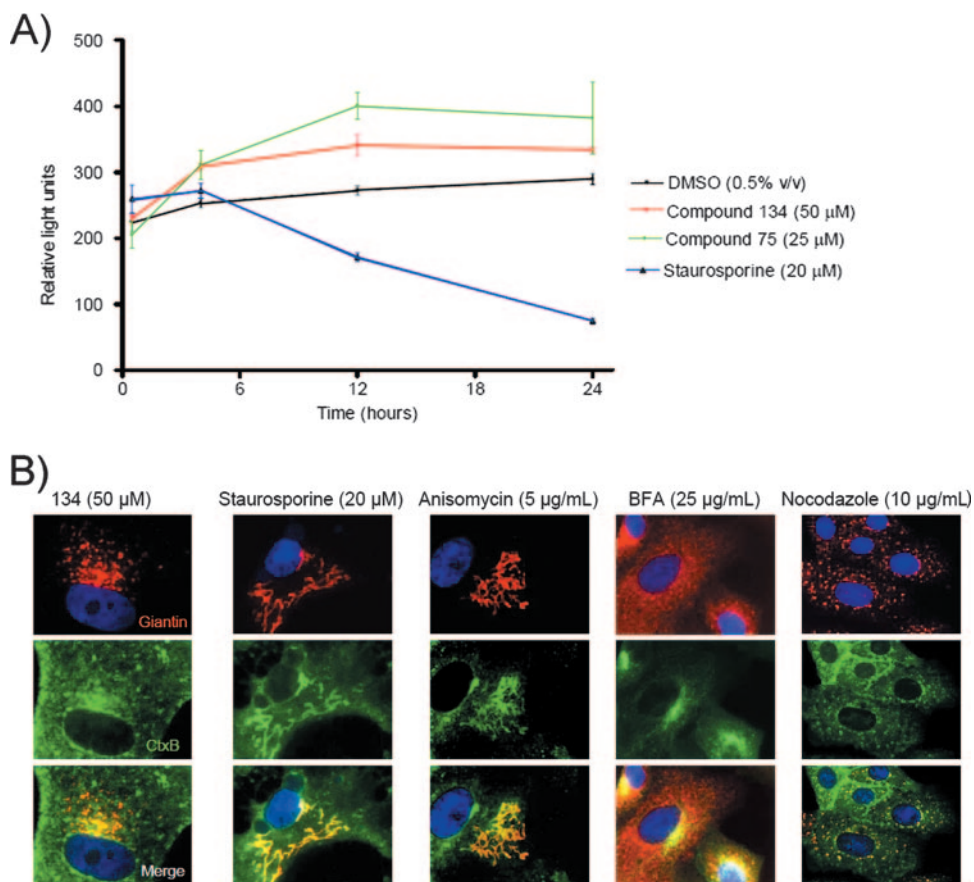


FIG. 3. The morphological and biochemical effects of compound treatment are distinct from those produced by apoptosis-inducing or Golgi-disturbing agents. (A) Compound treatment does not affect viability, as determined by intracellular ATP levels. Vero cells were incubated with compound 75, compound 134, staurosporine, or DMSO for as long as 24 h at 37°C at the indicated concentrations. ATP levels were determined by the CellTiter-Glo luminescent cell viability assay (see Materials and Methods). Luminescence (expressed as relative light units) is linearly related to ATP levels in viable cells. Results (means \pm standard deviations) are triplicate data for each time point from one representative experiment. (B) Compound 134 produces changes in Golgi morphology distinct from those generated by known apoptosis-inducing (staurosporine, anisomycin) or Golgi apparatus-disturbing (nocodazole, brefeldin A) agents. Vero cells were treated for 1 h with the specified compounds at the indicated concentrations prior to incubation with 1 μ g/ml Alexa Fluor 488-labeled CtXB at 4°C for 1 h. Toxin was internalized for 1 h at 37°C. Cells were fixed, permeabilized, and stained with an antibody against the Golgi marker giantin. Compound 75 produced a dispersal of the Golgi apparatus similar to that seen with compound 134 (see Fig. S3 in the supplemental material). Blue, nuclei. Images were obtained at \times 1,000 magnification.

HeLa cells (57). Other small-molecule compounds known to affect Golgi morphology include nocodazole (10), a microtubule-disrupting agent, and BFA, a known trafficking inhibitor that causes complete dispersal of the Golgi apparatus (24, 42). The morphological effects of compounds 75 and 134 on the Golgi apparatus were distinct from each of these (Fig. 3B). Thus, the effects on the Golgi apparatus, induced by these compounds as early as 30 min following compound treatment (see Fig. S3 in the supplemental material), were consistently distinct from the characteristic morphological and biochemical changes observed with known apoptosis-inducing and Golgi-disturbing agents.

As another means of determining and quantifying the effects of compounds 75 and 134 on toxin transport from early endosomes to the TGN, sulfation of a StxB construct bearing a tandem of C-terminal sulfation sites (StxB-Sulf₂) was evaluated. Sulfation of endogenous proteins occurs in the TGN, and sulfation of internalized StxB-Sulf₂ has shown that it traffics through this compartment (27). Trafficking of fluorescently

labeled StxB-Sulf₂ showed Golgi localization similar to that of native StxB labeled with Alexa Fluor 594 in untreated cells (Fig. 4A) and thus could serve as the basis for a suitable assay for toxin trafficking through the TGN. In agreement with its effect at an early stage in toxin trafficking, compound 75 decreased StxB sulfation to 47% of the level for compound-negative samples (Fig. 4B). By contrast, compound 134 modestly reduced sulfation (to 72% of the level for the control) over the 3-h incubation period. Sulfation of endogenous proteins, as assessed by total ³⁵S incorporation, was unaffected by compound treatment, implying that the compounds were not inhibiting sulfotransferase enzymatic activity (data not shown). Together with previous results, these results are consistent with compound 75 inhibiting transport at an early stage in endocytosis and compound 134 blocking transport at a post-recycling-endosome stage (including recycling-endosome-to-TGN transport).

Compounds 75 and 134 reversibly target toxin retrograde transport. Small-molecule compounds may act by reversible or

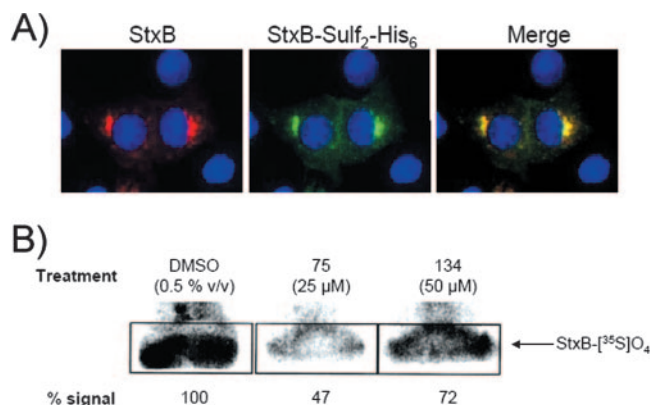


FIG. 4. Compounds 75 and 134 affect the trafficking of StxB through the TGN. (A) A StxB construct containing a tandem of sulfation sites and a histidine tag for purification (see Materials and Methods) was used to track StxB transport through the TGN in Vero cells. (B) The degree of sulfation of the StxB-Sulf₂ construct was determined as described in Materials and Methods. % signal, band density relative to the band signal in DMSO-treated cells from one representative experiment. Results are representative of two similar experiments.

irreversible mechanisms. In general, irreversible inhibitors act by covalent interaction with or modification of target molecules, such as through oxidation or acylation. Reversible compounds often act as competitive inhibitors of enzymatic activity or of protein-target interactions. Morphological effects on the Golgi apparatus produced by compound 75 or compound 134 treatment were found to be reversible. Following washout of the compounds, the Golgi apparatus reassembled in compound-treated cells at a time point at which BFA-treated cells maintained an altered Golgi morphology (Fig. 5A). More importantly, Vero cells lost protection against Stx following washout of either compound (Fig. 5B).

Effects of compounds on anterograde transport. The toxin-traffic pathway, proceeding from an early endosome to the ER via the Golgi apparatus, is almost the mirror inverse of the biosynthetic and secretory pathways. The degree of overlap between the retrograde and anterograde pathways, however, remains largely unresolved. Since no host molecules have been shown to traffic from endosomes all the way to the ER, the ability to track bacterial toxins and identify compounds that potentially block their transport allows us to specifically probe the retrograde pathway in its entirety.

To study the effects of these compounds on general anterograde transport, the sequential trafficking of a temperature-sensitive VSVG-GFP (*ts045*) fusion protein (19) in transiently transfected Vero cells was examined. Cells kept at 42°C showed that VSVG-GFP was confined to the ER, and a shift to 32°C allowed anterograde progression to the Golgi apparatus by 1 h (Fig. 6). Compounds 75 and 134 did not inhibit VSVG-GFP transport from the ER to the Golgi apparatus, as evidenced by colocalization of VSVG-GFP with TGN46 as early as 1 h following the shift to 32°C (Fig. 6). BFA has been shown to impede ER-to-Golgi apparatus transport (42), and cells treated with BFA showed a dispersed Golgi apparatus, with VSVG-GFP restricted to the ER, over the time course studied. We conclude that both compounds 75 and 134 do not inhibit ER-to-Golgi apparatus transport of VSVG-GFP, suggesting

that generalized anterograde transport mechanisms from the ER to the Golgi apparatus remain unaffected.

To equally monitor compound effects on the secretory pathway beyond the Golgi apparatus, secretion of a GFP construct bearing an amino-terminal NPY secretion signal (NPY-GFP) was assessed qualitatively and quantitatively. During the process of secretion, a portion of NPY-GFP is maintained in a compartment adjacent to and overlapping with the TGN (data not shown). In contrast to BFA and compound 75, compound 134 had a minimal effect on NPY-GFP secretion as judged by the immunofluorescence time course (see Fig. S4 in the supplemental material). Compound 75 partially impeded GFP secretion from the TGN-associated compartment, as evidenced by the persistence of GFP fluorescence as long as 1 h following cycloheximide treatment, at which time no GFP-positive cells were seen among control cells (see Fig. S4 in the supplemental material). An ELISA was developed to quantify the amounts of NPY-GFP secreted into the medium at various time points following cycloheximide treatment (to inhibit new protein synthesis). Mean absorbance values for control wells containing DMEM alone were subtracted from absorbance values for sample wells. Using this assay, we measured the effect of compound 134 (50 μ M) on GFP secretion. The level of GFP secretion by compound 134-treated cells was 86% of that by control (untreated) cells at 1 h and 89% of that by control cells at 2 h. (data not shown). Compound 75 (25 μ M) decreased post-Golgi secretion of NPY-GFP to 58% and 71% of that by control cells at 1 and 2 h, respectively (data not shown).

DISCUSSION

Using a luciferase-based assay that was adapted to an HTS for determining cell susceptibility to toxin-mediated inhibition of protein synthesis, we have screened a chemical library of small compounds and characterized two compounds that showed marked potency and selectivity against intracellular toxin transport. Both compounds demonstrated strong protective effects against Stx and ricin, and compound 75 was shown to protect equally against DT. We thus report two novel compounds demonstrating efficacy against multiple bacterial toxins, with toxin IC₅₀s nearly an order of magnitude greater than those reported previously using knockdown approaches for toxin inhibition (1, 8). More importantly, our results demonstrated that compounds 75 and 134 conferred toxin-protective effects by disrupting transport at distinct steps along the toxin-traffic pathway.

Screens at the ICCB facility have recently identified small-molecule inhibitors of *Toxoplasma gondii* invasion and *Vibrio cholerae* virulence. From a library of 12,160 compounds, 24 inhibitors of *Toxoplasma gondii* invasion were identified (5). These included compounds that inhibited host uptake of the organism as well as inhibitors of *Toxoplasma* gliding motility and microneme-based secretion. Effective doses of these compounds ranged from 3 to 100 μ M. Recently, a similar screen identified a small-molecule inhibitor of *Vibrio cholerae* virulence (20). A total of 50,000 compounds were screened, and 109 compounds that inhibited virulence factor expression were identified. Of these, a compound named virastatin inhibited the transcriptional regulator ToxT, thereby suppressing the

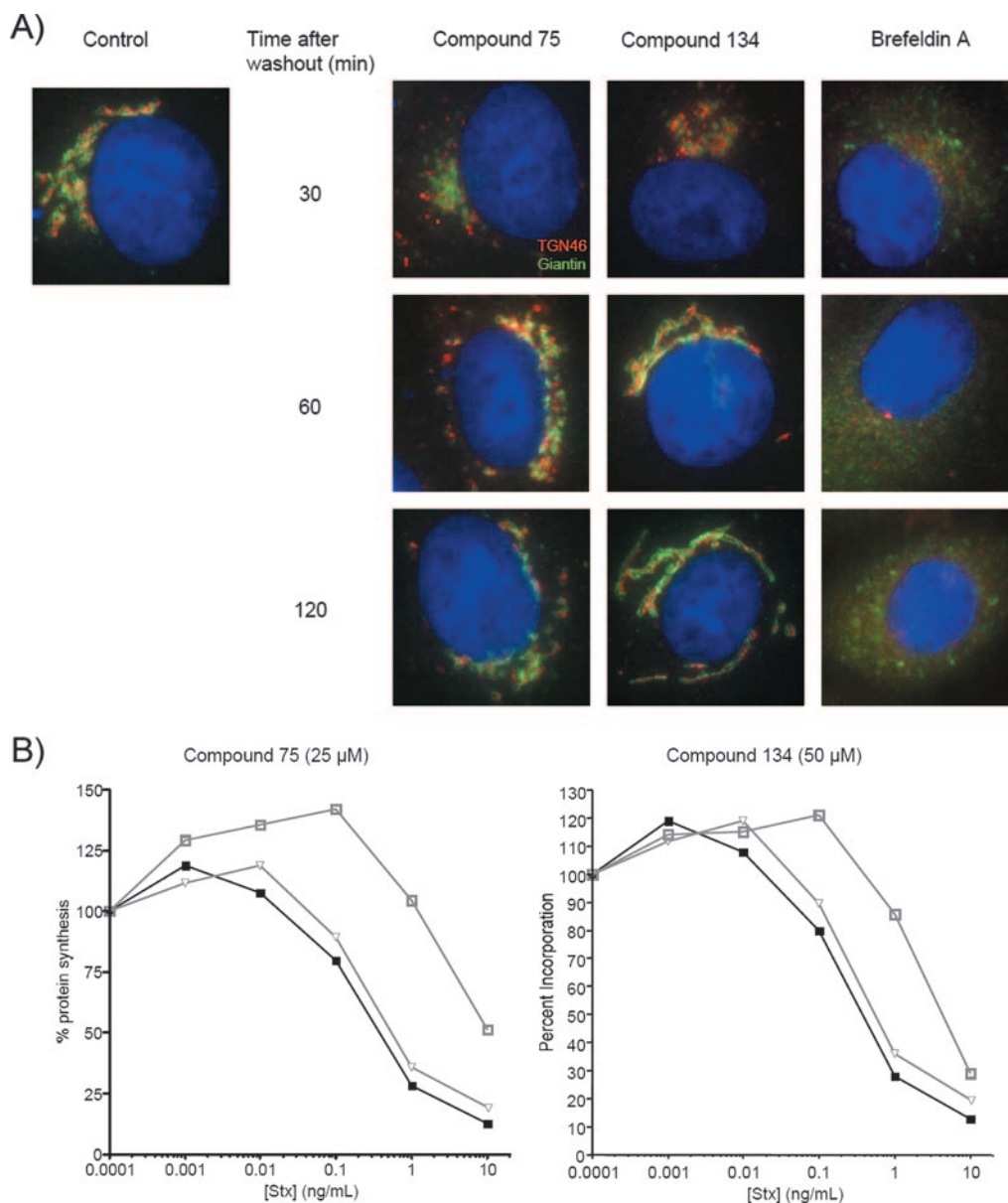


FIG. 5. Effects of compounds on Golgi structure are reversible. (A) Vero cells were treated with compound 75 (25 μM), compound 134 (50 μM), or BFA (25 μg/ml) for 1 h at 37°C, followed by a wash with prewarmed medium and an additional incubation at 37°C in medium alone for the indicated times. Cells were fixed, permeabilized, and stained with anti-giantin and anti-TGN46 antibodies. Control, cells treated with DMSO (0.5% [vol/vol]) and fixed 2 h after washing as were compound-treated cells. Blue, nuclei. Images were obtained at ×1,000 magnification. (B) Vero cells were pretreated with compounds for 1 h at 37°C, followed by a wash with prewarmed medium and an additional incubation at 37°C in medium alone for 2 h. Cells were then treated with Stx for 4 h and assessed for levels of protein synthesis by using the radioactive amino acid incorporation assay. Stx-response curves were generated as described in Materials and Methods. Black triangles, no treatment; gray squares, compound treatment alone; gray open triangles, compound treatment with washout.

expression of Ctx and the toxin-coregulated pilus. The MIC of virastatin against Ctx expression ranged from 3 to 40 μM, depending on the bacterial strain. Thus, recent screens underscore the utility of small-molecule assays in the identification of compounds that inhibit microbial virulence or block intracellular trafficking pathways.

Morphological analysis of compound-treated cells revealed dispersed Golgi apparatus-derived vesicles, but their pronounced toxin-protective effects were distinct from those of apoptosis-inducing or cytotoxic agents. The disrupted Golgi membranes

showed competent anterograde trafficking of VSVG-GFP and secretion of NPY-GFP in compound 134-treated cells, implying that this compound was preferentially targeting components of the retrograde pathway. Similar Golgi apparatus fragmentation has been observed in HeLa cells depleted of Cog3p, and the disrupted Golgi membranes were equally capable of anterograde trafficking of VSVG (65). Though it also exhibited a strong protective effect against toxin-mediated protein synthesis inhibition, compound 75 appeared to have a more pronounced effect on the post-Golgi trafficking of NPY-GFP. Nonetheless, the identifica-

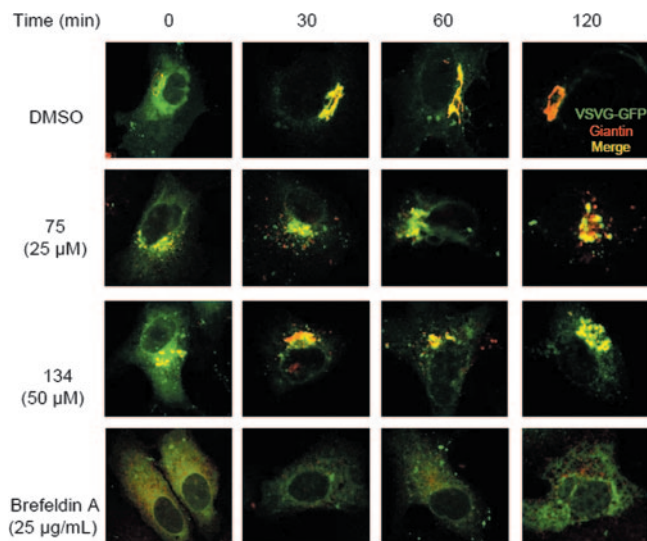


FIG. 6. Neither compound 75 or compound 134 inhibits anterograde transport from the ER to the Golgi apparatus. Anterograde transport of VSVG-GFP was assessed by immunofluorescence in Vero cells transiently transfected with pCDM8.1 expressing VSVG-GFP *ts045*, as described in Materials and Methods. Following fixation at the indicated times, cells were permeabilized and labeled with anti-TGN46. Yellow, colocalization of VSVG-GFP with TGN46. Images were obtained at $\times 1,000$ magnification.

tion of two compounds preferentially targeting the retrograde pathway could represent a useful tool in elucidating similarities and differences between anterograde and retrograde trafficking.

The retrograde transport of protein toxins is believed to occur exclusively from early and/or recycling endosomes (33), and it would be tempting to assume that toxins such as Stx, Ctx, and ricin subvert retrograde sorting pathways utilized by certain host proteins, such as acid hydrolase receptors (4), for endosome-to-TGN transport. Studies increasingly show that protein toxin transport to the TGN is not uniform (48), underscoring the complexity of retrograde pathways leading to a similar destination. A previous study examining toxin transport found that disruption of the Golgi apparatus by the expression of a temperature-sensitive mutant of ϵ -COP did not inhibit ricin transport in Chinese hamster ovary cells, and it was concluded that ricin was capable of bypassing the Golgi apparatus altogether through a normally inaccessible route (29). Though we cannot rule out the possibility that compound treatment is inducing an alternate toxin-trafficking pathway, it seems unlikely that the toxin is bypassing the Golgi apparatus to any appreciable extent in compound-treated cells, given that StxB and CtxB still traffic to the disrupted Golgi apparatus. Rather, our results indicate that an intact Golgi apparatus is required for efficient Stx trafficking and toxicity. The reversibility of compound effects on Golgi apparatus structure, concomitant with the loss of protection against Stx following Golgi apparatus reassembly, suggests that Stx transits in a retrograde manner through the Golgi apparatus, using a pathway that is equally responsible for maintaining Golgi apparatus structure.

In contrast to standard genetic approaches, which have been extensively employed to understand the retrograde pathways used by bacterial and plant toxins, small compounds provide an

informative chemical genetic method of studying intracellular toxin transport in a controlled and reversible manner (58). Pharmacological agents derived from small compounds have enhanced our understanding of the biology of retrograde transport and its implications for Golgi apparatus organization (10). Retrograde flow through the Golgi apparatus is believed to balance anterograde flow in order to establish a membrane equilibrium while maintaining Golgi apparatus polarity (2, 36, 51). It has been suggested that components regulating retrograde trafficking of glycolipid toxin receptors could also serve a role in the retrograde recycling of Golgi membranes (38, 61).

Indeed, it remains to be seen if the recycling of different resident Golgi proteins is being directly or indirectly targeted by protein toxins and, more importantly, whether the inhibitory effects of either or both of these compounds are targeting this host membrane recycling machinery. Future studies with covalently modified compounds will allow for the affinity purification of intracellular targets and the identification of host components involved in these processes. The roles of these intracellular targets in intracellular trafficking will elucidate our understanding of toxin subversion of retrograde, membrane recycling pathways. As the mechanisms underlying endocytic transport become clearer, the ability to manipulate and alter these pathways through small molecules will serve as an invaluable tool in probing both the retrograde and anterograde trafficking mechanisms.

ACKNOWLEDGMENTS

This work was supported by grant R01AI47900 from NIAID, by National Institutes of Health grant U54 AI057160 to the Midwest Regional Center of Excellence for Biodefense and Emerging Infectious Diseases Research (MRCE), and by an Investigator in Microbial Pathogenesis award to D.B.H. from the Burroughs Wellcome Foundation.

J.B.S. would like to personally dedicate the manuscript to the late Antero So, whose mentoring and expertise will be greatly missed in the scientific community.

REFERENCES

1. Abujarour, R. J., S. Dalal, P. I. Hanson, and R. K. Draper. 2005. p97 is in a complex with cholera toxin and influences the transport of cholera toxin and related toxins to the cytoplasm. *J. Biol. Chem.* **280**:15865–15871.
2. Allan, B. B., and W. E. Balch. 1999. Protein sorting by directed maturation of Golgi compartments. *Science* **285**:63–66.
3. Balint, G. S. 2004. Ricin—2004. *Orv. Hetil.* **145**:2379–2381. (In Hungarian.)
4. Bonifacino, J. S., and R. Rojas. 2006. Retrograde transport from endosomes to the trans-Golgi network. *Nat. Rev. Mol. Cell Biol.* **7**:568–579.
5. Carey, K. L., N. J. Westwood, T. J. Mitchison, and G. E. Ward. 2004. A small-molecule approach to studying invasive mechanisms of *Toxoplasma gondii*. *Proc. Natl. Acad. Sci. USA* **101**:7433–7438.
6. Casey, P. J., and A. G. Gilman. 1988. G protein involvement in receptor-effector coupling. *J. Biol. Chem.* **263**:2577–2580.
7. Chaudhary, V. K., Y. Jinno, D. FitzGerald, and I. Pastan. 1990. *Pseudomonas* exotoxin contains a specific sequence at the carboxyl terminus that is required for cytotoxicity. *Proc. Natl. Acad. Sci. USA* **87**:308–312.
8. Chen, A., R. J. AbuJarour, and R. K. Draper. 2003. Evidence that the transport of ricin to the cytoplasm is independent of both Rab6A and COPI. *J. Cell Sci.* **116**:3503–3510.
9. Chiu, R., L. Novikov, S. Mukherjee, and D. Shields. 2002. A caspase cleavage fragment of p115 induces fragmentation of the Golgi apparatus and apoptosis. *J. Cell Biol.* **159**:637–648.
10. Dinter, A., and E. G. Berger. 1998. Golgi-disturbing agents. *Histochem. Cell Biol.* **109**:571–590.
11. Elliott, S. P., M. Yu, H. Xu, and D. B. Haslam. 2003. Forssman synthetase expression results in diminished Shiga toxin susceptibility: a role for glycolipids in determining host-microbe interactions. *Infect. Immun.* **71**:6543–6552.
12. El Meskini, R., L. Jin, R. Marx, A. Bruzzaniti, J. Lee, R. Emeson, and R. Mains. 2001. A signal sequence is sufficient for green fluorescent protein to be routed to regulated secretory granules. *Endocrinology* **142**:864–873.
13. Endo, Y., and K. Tsurugi. 1986. Mechanism of action of ricin and related toxic lectins on eukaryotic ribosomes. *Nucleic Acids Symp. Ser.* **17**:187–190.

14. **Falguieres, T., F. Mallard, C. Baron, D. Hanau, C. Lingwood, B. Goud, J. Salamero, and L. Johannes.** 2001. Targeting of Shiga toxin B-subunit to retrograde transport route in association with detergent-resistant membranes. *Mol. Biol. Cell* **12**:2453–2468.
15. **Falnes, P. O., and K. Sandvig.** 2000. Penetration of protein toxins into cells. *Curr. Opin. Cell Biol.* **12**:407–413.
16. **Garred, O., B. van Deurs, and K. Sandvig.** 1995. Furin-induced cleavage and activation of Shiga toxin. *J. Biol. Chem.* **270**:10817–10821.
17. **Girod, A., B. Storrie, J. C. Simpson, L. Johannes, B. Goud, L. M. Roberts, J. M. Lord, T. Nilsson, and R. Pepperkok.** 1999. Evidence for a COP-I-independent transport route from the Golgi complex to the endoplasmic reticulum. *Nat. Cell Biol.* **1**:423–430.
18. **Guidi-Rontani, C., M. Weber-Levy, M. Mock, and V. Cabiiaux.** 2000. Translocation of *Bacillus anthracis* lethal and oedema factors across endosome membranes. *Cell. Microbiol.* **2**:259–264.
19. **Hirschberg, K., and J. Lippincott-Schwartz.** 1999. Secretory pathway kinetics and in vivo analysis of protein traffic from the Golgi complex to the cell surface. *FASEB J.* **13**(Suppl. 2):S251–S256.
20. **Hung, D. T., E. A. Shakhovich, E. Pierson, and J. J. Mekalanos.** 2005. Small-molecule inhibitor of *Vibrio cholerae* virulence and intestinal colonization. *Science* **310**:670–674.
21. **Iversen, T. G., G. Skretting, A. Llorente, P. Nicoziani, B. van Deurs, and K. Sandvig.** 2001. Endosome to Golgi transport of ricin is independent of clathrin and of the Rab9- and Rab11-GTPases. *Mol. Biol. Cell* **12**:2099–2107.
22. **Johannes, L., D. Tenza, C. Antony, and B. Goud.** 1997. Retrograde transport of KDEL-bearing B-fragment of Shiga toxin. *J. Biol. Chem.* **272**:19554–19561.
23. **Kabir, J., M. Lobo, and I. Zachary.** 2002. Staurosporine induces endothelial cell apoptosis via focal adhesion kinase dephosphorylation and focal adhesion disassembly independent of focal adhesion kinase proteolysis. *Biochem. J.* **367**:145–155.
24. **Kojio, S., H. Zhang, M. Ohmura, F. Gondaira, N. Kobayashi, and T. Yamamoto.** 2000. Caspase-3 activation and apoptosis induction coupled with the retrograde transport of shiga toxin: inhibition by brefeldin A. *FEMS Immunol. Med. Microbiol.* **29**:275–281.
25. **Kok, J. W., T. Babia, C. M. Filipeanu, A. Nelemans, G. Egea, and D. Hoekstra.** 1998. PDMP blocks brefeldin A-induced retrograde membrane transport from Golgi to ER: evidence for involvement of calcium homeostasis and dissociation from sphingolipid metabolism. *J. Cell Biol.* **142**:25–38.
26. **Kumar, P., N. Ahuja, and R. Bhatnagar.** 2002. Anthrax edema toxin requires influx of calcium for inducing cyclic AMP toxicity in target cells. *Infect. Immun.* **70**:4997–5007.
27. **Lauvrak, S. U., M. L. Torgersen, and K. Sandvig.** 2004. Efficient endosome-to-Golgi transport of Shiga toxin is dependent on dynamin and clathrin. *J. Cell Sci.* **117**:2321–2331.
28. **Lemichiez, E., M. Bomsel, G. Devilliers, J. R. Murphy, E. V. Lukianov, S. Olsnes, and P. Boquet.** 1997. Membrane translocation of diphtheria toxin fragment A exploits early to late endosome trafficking machinery. *Mol. Microbiol.* **23**:445–457.
29. **Llorente, A., S. U. Lauvrak, B. van Deurs, and K. Sandvig.** 2003. Induction of direct endosome to endoplasmic reticulum transport in Chinese hamster ovary (CHO) cells (LdlF) with a temperature-sensitive defect in epsilon-COP. *J. Biol. Chem.* **278**:35850–35855.
30. **Lord, J. M., D. C. Smith, and L. M. Roberts.** 1999. Toxin entry: how bacterial proteins get into mammalian cells. *Cell. Microbiol.* **1**:85–91.
31. **Machamer, C. E.** 2003. Golgi disassembly in apoptosis: cause or effect? *Trends Cell Biol.* **13**:279–281.
32. **Mallard, F., and L. Johannes.** 2003. Shiga toxin B-subunit as a tool to study retrograde transport. *Methods Mol. Med.* **73**:209–220.
33. **Mallard, F., B. L. Tang, T. Galli, D. Tenza, A. Saint-Pol, X. Yue, C. Antony, W. Hong, B. Goud, and L. Johannes.** 2002. Early/recycling endosomes-to-TGN transport involves two SNARE complexes and a Rab6 isoform. *J. Cell Biol.* **156**:653–664.
34. **Mesa, R., J. Magadan, A. Barbieri, C. Lopez, P. D. Stahl, and L. S. Mayorga.** 2005. Overexpression of Rab22a hampers the transport between endosomes and the Golgi apparatus. *Exp. Cell Res.* **304**:339–353.
35. **Milne, J. C., and R. J. Collier.** 1993. pH-dependent permeabilization of the plasma membrane of mammalian cells by anthrax protective antigen. *Mol. Microbiol.* **10**:647–653.
36. **Mironov, A. A., P. Weidman, and A. Luini.** 1997. Variations on the intracellular transport theme: maturing cisternae and trafficking tubules. *J. Cell Biol.* **138**:481–484.
37. **Morinaga, N., Y. Kaihou, N. Vitale, J. Moss, and M. Noda.** 2001. Involvement of ADP-ribosylation factor 1 in cholera toxin-induced morphological changes of Chinese hamster ovary cells. *J. Biol. Chem.* **276**:22838–22843.
38. **Nichols, B. J., A. K. Kenworthy, R. S. Polishchuk, R. Lodge, T. H. Roberts, K. Hirschberg, R. D. Phair, and J. Lippincott-Schwartz.** 2001. Rapid cycling of lipid raft markers between the cell surface and Golgi complex. *J. Cell Biol.* **153**:529–541.
39. **Obrig, T. G., T. P. Moran, and J. E. Brown.** 1987. The mode of action of Shiga toxin on peptide elongation of eukaryotic protein synthesis. *Biochem. J.* **244**:287–294.
40. **Obrig, T. G., T. P. Moran, and R. J. Colinas.** 1985. Ribonuclease activity associated with the 60S ribosome-inactivating proteins ricin A, phytolaccin and Shiga toxin. *Biochem. Biophys. Res. Commun.* **130**:879–884.
41. **Oh, K. J., L. Senzel, R. J. Collier, and A. Finkelstein.** 1999. Translocation of the catalytic domain of diphtheria toxin across planar phospholipid bilayers by its own T domain. *Proc. Natl. Acad. Sci. USA* **96**:8467–8470.
42. **Orlandi, P. A., P. K. Curran, and P. H. Fishman.** 1993. Brefeldin A blocks the response of cultured cells to cholera toxin. Implications for intracellular trafficking in toxin action. *J. Biol. Chem.* **268**:12010–12016.
43. **Puthenveedu, M. A., and A. D. Linstedt.** 2001. Evidence that Golgi structure depends on a p115 activity that is independent of the vesicle tether components giantin and GM130. *J. Cell Biol.* **155**:227–238.
44. **Rechsteiner, M.** 1990. PEST sequences are signals for rapid intracellular proteolysis. *Semin. Cell Biol.* **1**:433–440.
45. **Reisbig, R., S. Olsnes, and K. Eiklid.** 1981. The cytotoxic activity of *Shigella* toxin. Evidence for catalytic inactivation of the 60 S ribosomal subunit. *J. Biol. Chem.* **256**:8739–8744.
46. **Sandvig, K., O. Garred, K. Prydz, J. V. Kozlov, S. H. Hansen, and B. van Deurs.** 1992. Retrograde transport of endocytosed Shiga toxin to the endoplasmic reticulum. *Nature* **358**:510–512.
47. **Sandvig, K., S. Grimmer, T. G. Iversen, K. Rodal, M. L. Torgersen, P. Nicoziani, and B. van Deurs.** 2000. Ricin transport into cells: studies of endocytosis and intracellular transport. *Int. J. Med. Microbiol.* **290**:415–420.
48. **Sandvig, K., and B. van Deurs.** 2002. Transport of protein toxins into cells: pathways used by ricin, cholera toxin and Shiga toxin. *FEBS Lett.* **529**:49–53.
49. **Schmitz, A., H. Herrgen, A. Winkler, and V. Herzog.** 2000. Cholera toxin is exported from microsomes by the Sec61p complex. *J. Cell Biol.* **148**:1203–1212.
50. **Sherwood, A. L., and E. H. Holmes.** 1992. Brefeldin A induced inhibition of de novo globo- and neolacto-series glycolipid core chain biosynthesis in human cells. Evidence for an effect on β 1 \rightarrow 4 galactosyltransferase activity. *J. Biol. Chem.* **267**:25328–25336.
51. **Shorter, J., and G. Warren.** 2002. Golgi architecture and inheritance. *Ann. Rev. Cell Dev. Biol.* **18**:379–420.
52. **Simpson, J. C., L. M. Roberts, K. Romisch, J. Davey, D. H. Wolf, and J. M. Lord.** 1999. Ricin A chain utilises the endoplasmic reticulum-associated protein degradation pathway to enter the cytosol of yeast. *FEBS Lett.* **459**:80–84.
53. **Stenmark, H., and V. M. Olkkonen.** 2001. The Rab GTPase family. *Genome Biol.* **2**:REVIEWS3007.
54. **Stryer, L.** 1983. Transducin and the cyclic GMP phosphodiesterase: amplifier proteins in vision. *Cold Spring Harbor Symp. Quant. Biol.* **48**:841–852.
55. **Sutton, C. A., M. J. Ares, and R. L. Hallberg.** 1978. Cycloheximide resistance can be mediated through either ribosomal subunit. *Proc. Natl. Acad. Sci. USA* **75**:3158–3162.
56. **Tsai, B., C. Rodighiero, W. I. Lencer, and T. A. Rapoport.** 2001. Protein disulfide isomerase acts as a redox-dependent chaperone to unfold cholera toxin. *Cell* **104**:937–948.
57. **Tscherne, J. S., and S. Pestka.** 1975. Inhibition of protein synthesis in intact HeLa cells. *Antimicrob. Agents Chemother.* **8**:479–487.
58. **Ward, G. E., K. L. Carey, and N. J. Westwood.** 2002. Using small molecules to study big questions in cellular microbiology. *Cell. Microbiol.* **4**:471–482.
59. **White, J., L. Johannes, F. Mallard, A. Girod, S. Grill, S. Reinsch, P. Keller, B. Tzschaschel, A. Echard, B. Goud, and E. H. Stelzer.** 1999. Rab6 coordinates a novel Golgi to ER retrograde transport pathway in live cells. *J. Cell Biol.* **147**:743–760. (Erratum, **148**:205, 2000.)
60. **Wilcke, M., L. Johannes, T. Galli, V. Mayau, B. Goud, and J. Salamero.** 2000. Rab11 regulates the compartmentalization of early endosomes required for efficient transport from early endosomes to the trans-Golgi network. *J. Cell Biol.* **151**:1207–1220.
61. **Yoshino, A., S. R. Setty, C. Poynton, E. L. Whiteman, A. Saint-Pol, C. G. Burd, L. Johannes, E. L. Holzbaur, M. Koval, J. M. McCaffery, and M. S. Marks.** 2005. tGolgin-1 (p230, golgin-245) modulates Shiga-toxin transport to the Golgi and Golgi motility towards the microtubule-organizing centre. *J. Cell Sci.* **118**:2279–2293.
62. **Yu, M., and D. B. Haslam.** 2005. Shiga toxin is transported from the endoplasmic reticulum following interaction with the luminal chaperone HEDJ/ERdj3. *Infect. Immun.* **73**:2524–2532.
63. **Yu, M., R. H. Haslam, and D. B. Haslam.** 2000. HEDJ, an Hsp40 co-chaperone localized to the endoplasmic reticulum of human cells. *J. Biol. Chem.* **275**:24984–24992.
64. **Zhao, L., and D. B. Haslam.** 2005. A quantitative and highly sensitive luciferase-based assay for bacterial toxins that inhibit protein synthesis. *J. Med. Microbiol.* **54**:1023–1030.
65. **Zolov, S. N., and V. V. Lupashin.** 2005. Cog3p depletion blocks vesicle-mediated Golgi retrograde trafficking in HeLa cells. *J. Cell Biol.* **168**:747–759.